PERGAMON

International Journal of Solids and Structures 37 (2000) 1145–1164

INTERNATIONAL JOURNAL OF SOLIDS and STRUCTURES

www.elsevier.com/locate/ijsolstr

A one-dimensional continuum model for thermoelectric phase transformations in ferroelectrics

Sang-Joo Kim*

Department of Mechanical Engineering, University of Seoul, 90 Cheonnong-dong, Tongdaemun-gu, Seoul 130-743, South Korea

Received 4 February 1998; in revised form 30 July 1998; accepted 10 August 1998

Abstract

In this paper we construct an explicit one-dimensional constitutive model that is capable of describing some aspects of the thermoelectrical response of a ferroelectric material. The model consists of a Helmholtz free-energy function, a kinetic relation and a nucleation criterion. The free-energy is associated with a three-well potential energy function; the kinetic relation is taken to be a simple linear function of driving traction; and nucleation is assumed to occur at a critical value of driving traction. The predictions of the model in various quasi-static thermoelectrical loadings are examined and compared with experimental observations.

1. Introduction

Many crystalline solids may change their crystal structure or phase in response to various external stimuli. One phase is preferred under a certain condition of stimulation and another phase is favored in a different condition. The stimuli can be mechanical, thermal, electric, magnetic or optical. A ferroelectric crystal, which is one of those phase-transforming materials, undergoes a structural transformation by an application of electro-thermomechanical loads. For example, it transforms phase at a critical temperature called the Curie point in the absence of electrical and mechanical loadings. Above the temperature, it has a non-polar structure called paraelectric; below it, a polar structure called ferroelectric. The polarization below the Curie point with no applied electric field and stress is called spontaneous polarization. The magnitude of spontaneous polarization diminishes as temperature increases and finally at the Curie point it vanishes. The direction of spontaneous polarization can be reversed by an application of electric field and this is often called polarization switching or polarization reversal.

* Fax: 011 822 2248-5100.
E-mail address: sjkim@seoul.uos.ac.kr (S.-J. Kim).

0020-7683/00/$ - see front matter
PII: S0020-7683(98)00251-0

In order to model a phase transformation in a ferroelectric material, the potential energy function that characterizes the material, as a function of polarization intensity, should have multiple energy-wells for certain ranges of electric field, stress and temperature and each energy-well is identified with a phase (or a variant of a phase) of the material. The process of phase transformation corresponds to a movement of a material particle from one energy-well to another. Therefore, a complete constitutive theory that describes the behavior of such materials consists of a Helmholtz free-energy function which describes the response of each individual phase, a nucleation criterion which signals the conditions under which the transition from one phase to another commences and a kinetic law which characterizes the rate at which this transition progresses.

Recently some continuum models for polarization reversals or paraelectric–ferroelectric transformations have been suggested. Jiang (1993) regarded a ferroelectric material as a thermoelastic polarizable solid and constructed a one-dimensional energy function capable of describing a paraelectric–ferroelectric phase transformation under the influence of electrical or thermomechanical loads. His energy function consists of several polynomials including the terms up to the sixth power of polarization intensity in order to have five monotonic branches in the electric field–polarization intensity curves. He also suggested a kinetic relation controlling the velocity of phase boundary and a nucleation criterion based on a critical value of driving traction. The model is generalized to a three-dimensional one by Jiang (1994a). Hwang et al. (1995) carried out experiments on PLZT ceramics and predicted experimental observations by computing the behavior of an individual grain based on a Preisach hysteresis model and averaging the response of individual grains. Kim and Jiang (1996) showed that the generation of microcracks inside ferroelectrics may be a reason for the so-called electric fatigue which refers the degradation of material properties after a large number of cycles of applied electric field. McMeeking and Hwang (1997) studied the potential energy of an infinite homogeneous piezoelectric loaded body containing a single ellipsoidal transforming inhomogeneity and constructed criteria for the first crystallite to switch in an unpolarized polycrystalline ferroelectric.

In the present paper we focus on an electric field- or temperature-induced phase transformation in a ferroelectric material and construct a complete one-dimensional constitutive model. A ferroelectric material is regarded as a thermopolarizable solid which is characterized by a Helmholtz free-energy function. The Helmholtz free energy function here, depending on the polarization intensity and temperature, has three energy-wells corresponding to the three phases of the material—a paraelectric phase and two variants of ferroelectric phase. As in Kim and Abeyaratne (1995) and Jiang (1993), the nucleation criterion utilized in the present study is based on a critical value of driving traction. The number of interfaces that can occur in the bar is controlled by the nucleation criterion. For the particular criterion adopted here, this number is small, usually one, so that if many interfaces are to be allowed, we would have to modify this ingredient of the present model. The kinetic law that we adopt here is based on the model of Jiang (1993); the velocity of phase boundary is taken to be linearly proportional to driving traction.

Although we limit our attention here to purely thermoelectrical quasi-static processes, one of the primary motivations of the present model is the possibility that it may prove amenable to a study of thermal effects (see Kim and Abeyaratne, 1995) and electric fatigue (see Kim and Jiang, 1996) in ferroelectric materials.

In Section 2 we briefly outline the basic one-dimensional thermoelectrical framework within which the model will be constructed. In Section 3 we construct the three-well energy function and discuss the stability of the various phases. Next, in Section 4 we suggest the nucleation criterion and kinetic relation. In Section 5 we carry out a number of simulations and compare them with experimental observations.

Finally, a note on terminology: for simplicity of presentation we shall sometimes speak of the ‘two

phases' rather than the 'two variants'; similarly we shall often use the term 'phase boundary' generically to refer to an interface between two variants (which ought to be called a domain boundary).

2. Preliminaries

In this section we describe some relevant concepts from the continuum theory of thermoelectrical processes within a one-dimensional setting. Here we consider a uniform bar with length L, cross-sectional area A and mass density ρ in a reference configuration. Suppose that the bar is located within a heat bath whose temperature is θ. The specimen is viewed as a one-dimensional bar that occupies the interval $[0, L]$ of the x-axis in this configuration. The bar is placed between and in contact with two electrode plates of a condenser that provides electromotive force; see Fig. 1. The bar is composed of a ferroelectric crystal whose polar axis is normal to the electrodes. Therefore, a particle in the bar is polarized either parallel or antiparallel to the applied electric field and the polarization intensity may be described by a scalar field $p(x)$. The electric field away from the edges of the condenser plates is normal to the plates and its scalar magnitude is the applied voltage divided by the distance between the electrodes.

The bar is modeled as a thermopolarizable solid whose bulk behavior may be characterized by its Helmholtz free-energy per unit mass $\psi(p, \theta)$, where p is polarization intensity and θ is temperature. The electric field e and specific entropy η at a particle are then constitutively related to p and θ through

$$e = \rho\psi_p(p, \theta),$$

$$\eta = -\psi_\theta(p, \theta). \tag{1}$$

The potential energy per unit reference volume $G(p; \theta, e)$ of the material is defined by

$$G(p; \theta, e) = \rho\psi(p, \theta) - ep, \tag{2}$$

and its value at an extremum of $G(\bullet; \theta, e)$ coincides with the Gibbs free energy per unit reference volume

$$g(p, \theta) = \rho\psi(p, \theta) - \rho\psi_p(p, \theta)p. \tag{3}$$

In order to model a material that can undergo a thermoelectric phase transition, the function $G(\bullet; \theta, e)$ should have multiple local minima ('energy wells') when the temperature and electric field take on suitable values. The corresponding Helmholtz free-energy potential $\psi(\bullet, \theta)$ will be non-convex and the electric field–polarization curve characterized by $e = \rho\psi_p(p, \theta)$ will be non-monotonic. In this theory, each local minimum of the potential energy function G and therefore, each branch with positive slope of the electric field–polarization curve, is identified with a different (metastable) phase of the material.

Being concerned with two-phase equilibrium states, we suppose that $G(\bullet; \theta, e)$ has at least two local minima corresponding to a given electric-field e and temperature θ and let $p = \bar{p} = \bar{p}(\theta, e), \eta = \bar{\eta} =$

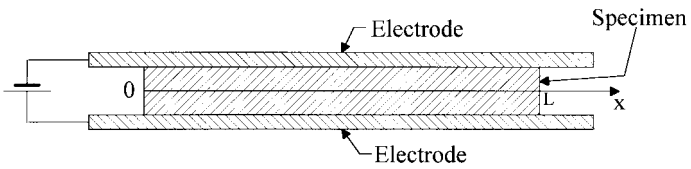

Fig. 1. The ferroelectric specimen.

$\bar{\eta}(\theta, e)$ and $p = \overset{+}{p} = \overset{+}{p}(\theta, e)$, $\eta = \overset{+}{\eta} = \overset{+}{\eta}(\theta, e)$ denote the values of polarization intensity and entropy at these two energy wells. Then the polarization intensity and entropy at a particle that is subjected to this θ and e could be either $\bar{p}$, $\bar{\eta}$ or $\overset{+}{p}$, $\overset{+}{\eta}$ depending on which energy-well (i.e. phase) the particle is in. The interface $x = s$ at which the polarization intensity and entropy jump is called a phase boundary. The phase boundary separates two distinct phases of the material. If there is only one phase boundary at $x = s$ in the bar, then the average intensity p_a of polarization of the bar is given by

$$p_a = \frac{s}{L}\,\bar{p}(\theta, e) + \frac{L - s}{L}\overset{+}{p}(\theta, e). \tag{4}$$

We now consider quasi-static processes, which mean one-parameter families of equilibrium states with the parameter being the time t. The electric field and the heat bath temperature are now functions of time: $e = e(t)$, $\theta = \theta(t)$ and in a two-phase quasi-static process, one also has $\overset{\pm}{p} = \overset{\pm}{p}(t)$, $\overset{\pm}{\eta} = \overset{\pm}{\eta}(t)$, $s = s(t)$ and $p_a = p_a(t)$.

Let

$$\hat{\varepsilon}(p, \theta) = \hat{\psi}(p, \theta) + \theta\hat{\eta}(p, \theta) \tag{5}$$

be the internal energy of the material, measured per unit mass. For the two-phase quasi-static process, we set $\overset{\pm}{\varepsilon}(t) = \hat{\varepsilon}(\overset{\pm}{p}(t), \theta(t))$ so that the total internal energy in the bar at time t is

$$E(t) = \rho A\left[\bar{\varepsilon}(t)s(t) + \overset{+}{\varepsilon}(t)(L - s(t))\right]. \tag{6}$$

If $Q(t)$ is the rate at which heat is supplied to the bar at time t, the first law of thermodynamics requires that

$$\dot{E}(t) = e(t)AL\dot{p}_a(t) + Q(t), \tag{7}$$

where we use a superposed dot to denote the time derivative of the corresponding variable.

In the present setting, the second law of thermodynamics asserts that

$$\Gamma(t) \equiv \dot{H}(t) - \frac{Q(t)}{\theta(t)} \geqslant 0, \tag{8}$$

where

$$H(t) = \rho A\left[\bar{\eta}(t)s(t) + \overset{+}{\eta}(t)(L - s(t))\right] \tag{9}$$

is the total entropy in the bar and Γ(t) is, therefore, the rate of entropy production. Eliminating $Q(t)$ between (7) and (8) and invoking (1)–(6), (9) yields the following alternative representation for Γ(t):

$$\Gamma(t) = f(t)A\dot{s}(t)/\theta(t), \tag{10}$$

where

$$f = G(\overset{+}{p}; \theta, e) - G(\bar{p}; \theta, e); \tag{11}$$

f is known as the 'driving traction' acting on the phase boundary. A discussion of the notion of driving traction in a general three-dimensional setting may be found in Abeyaratne and Knowles (1990) and Jiang (1994b). The second law of thermodynamics thus requires that the following dissipation inequality hold:

$$f\dot{s} \geqslant 0. \tag{12}$$

If $G(\overset{+}{p};\theta,e) > G(\bar{p};\theta,e)$, then from (2.11) f is positive and so according to (12) $\dot{s} \geqslant 0$; thus, if the phase boundary propagates, it moves into the positive side and thereby transforms particles from $(\overset{+}{p},\theta)$ to $(\bar{p},\theta)$. The phase boundary moves in the direction of decreasing the Gibbs energy of the bar and in this sense the material prefers the smaller minimum of G. This is also true in the reverse case when $G(\overset{+}{p};\theta,e) < G(\bar{p};\theta,e)$. Therefore, the phase associated with the lowest energy-well is being referred to as the stable phase. If the driving traction f happens to vanish, one speaks of the states $(\overset{+}{p},\theta)$, and $(\bar{p},\theta)$ as being in 'phase equilibrium' and of the quasi-static process as taking place 'reversely'. In this case (12) permits $\dot{s}$ to have either sign and the phase boundary may move in either direction.

Combining (8)–(10) gives the following representation for $Q(t)$:

$$Q(t) = \rho A\theta(t)\left\{\frac{\mathrm{d}\bar{\eta}}{\mathrm{d}t}s(t) + \frac{\mathrm{d}\overset{+}{\eta}(t)}{\mathrm{d}t}(L - s(t))\right\} - \left\{\frac{f(t)}{\rho} + \lambda(t)\right\}\rho A\dot{s}, \tag{13}$$

where

$$\lambda(t) = \theta(t)\left\{\overset{+}{\eta}(t) - \bar{\eta}(t)\right\}. \tag{14}$$

The contents of the second brace $f/\rho + \lambda$ in (13) represents the heat generated when a unit of material changes phase from $(\overset{+}{p},\theta)$, to $(\bar{p},\theta)$. In particular, λ is the heat generated from the difference in the values of specific entropy of phases across the phase boundary and is called *latent heat*. If the phase change occurs under conditions of phase equilibrium, then $f = 0$ and the heat generated is λ.

In (4) there are only two of the four functions of time known and an additional equation should be supplied to completely describe the behavior of the bar. Such supplementary information is provided by the kinetic relation controlling the evolution of the phase boundary. If we assume that the propagation of a phase boundary depends only on the states $(\overset{+}{p},\theta)$, and $(\bar{p},\theta)$ on either side of the interface, then its velocity $\dot{s}$ would have the from $\dot{s} = v(\bar{p},\overset{+}{p},\theta)$, where the kinetic response function v is determined by the material. Alternatively, the function v can be expressed by using (1) and (11) in the form

$$\dot{s} = V(f,\theta). \tag{15}$$

No further information on the kinetic response function V is available from the basic principles of the continuum theory. Explicit examples of V must be supplied by suitable constitutive modeling, for example, see Abeyaratne and Knowles (1993).

We shall consider quasi-static processes in which the entire bar is in a single phase for an initial interval of time and in two-phase states for subsequent times. A nucleation criterion provides information on when and where the transition from the single-phase to the two-phase configurations occurs. In this paper we follow the model suggested by Abeyaratne and Knowles (1993) and Abeyaratne et al. (1994), which is that the nucleation of a new phase occurs at the ends of the bar when the driving traction f at the incipient phase boundary would be at least as a certain materially-determined critical value.

3. Helmholtz free-energy function

In this section we construct explicitly a particular Helmholtz free-energy function $\psi(p,\theta)$ that is capable of modeling certain features of thermoelectric phase transformations. Our intent is to supply a model which yields a simple piecewise linear electric field–polarization–temperature relation and may be used to investigate thermal effects in polarization switchings. The model turns out to have a great

analogy to the model developed by Abeyaratne et al. (1994) to study a thermomechanical phase transformation in shape memory alloys.

3.1. Construction of Helmholtz free-energy function

We construct an explicit three-well Helmholtz free-energy function $\psi(p, \theta)$ that characterizes the response of a multi-phase material. The three energy-wells are viewed as corresponding to a paraelectric phase and two variants of ferroelectric phase. Recall first that the inverse susceptibility at constant temperature χ, pyroelectric coefficient β and specific heat at constant polarization intensity c of a thermopolarizable material are related to $\psi(p, \theta)$ through

$$\rho\psi_{pp}(p, \theta) = \chi, \quad -\frac{\psi_{p\theta}(p, \theta)}{\psi_{pp}(p, \theta)} = \beta, \quad -\theta\psi_{\theta\theta}(p, \theta) = c. \tag{16}$$

Thus, if χ, β and c are constant on some domain of the (p, θ)-plane, then by integrating (16) one finds that

$$\rho\psi(p, \theta) = (\chi/2)(p - p_*)^2 - \chi\beta p\theta + \rho c\theta\big(1 - \log(\theta/\theta_*)\big) + \rho\psi_* \tag{17}$$

on that domain, where p_*, θ_* and ψ_* are constants.

Consider a material which exists in a high temperature phase paraelectric (P) and as two variants (F^+ and F^-) of a low-temperature phase ferroelectric. Suppose for simplicity that the paraelectric P and both ferroelectric variants F^+ and F^- have the same constant inverse susceptibility $\chi > 0$ and the same constant specific heat $c > 0$ but different pyroelectric coefficient 0, $-\beta$ and $\beta > 0$, respectively. (The model that follows can be readily generalized to describe the case wherein the different phases have different but constant material properties.) By (17), the Helmholtz free-energy function $\psi(p, \theta)$ associated with this material must have the form

$$\rho\psi(p, \theta) = \begin{cases} (\chi/2)(p - p_1)^2 + \rho c\theta\big(1 - \log(\theta/\theta_1)\big) + \rho\psi_1 & \text{on } D_1, \\ (\chi/2)(p - p_2)^2 + \chi\beta p\theta + \rho c\theta\big(1 - \log(\theta/\theta_2)\big) + \rho\psi_2 & \text{on } D_2, \\ (\chi/2)(p - p_3)^2 - \chi\beta p\theta + \rho c\theta\big(1 - \log(\theta/\theta_3)\big) + \rho\psi_3 & \text{on } D_3, \end{cases} \tag{18}$$

where ρ is the mass density of the material in the reference configuration and p_i, θ_i, ψ_i, $i = 1, 2, 3$, are nine additional material constants whose physical significance will be made clear in what follows. The regions D_1, D_2, and D_3 of the (p, θ)-plane on which the three expressions in (18) hold are the regions on which the respective phase P, F^+ and F^- exist; they are assumed to take the form shown in Fig. 2, where in particular the boundaries of P, F^+ and F^- have been taken to be straight lines. The temperature levels θ_m and θ_M denote two critical values of temperature: for $\theta > \theta_M$ the material exists only in its paraelectric form, whereas for $\theta < \theta_m$ the material exists only in its ferroelectric forms. Throughout this paper we will restrict attention to temperatures less than θ_M.

We now impose a number of restrictions on the potential function G in order that it may properly model the electric field-free response of the material we have in mind. Since G and the Helmholtz free-energy function ψ coincide when the electric field vanishes, any characteristic to be assigned to G at $e = 0$ could be equivalently imposed on ψ. First, we assume that there is a special temperature θ_T between θ_m and θ_M such that, when $e = 0$, all three phase F^-, P and F^+ are stable. Thus, the function $\psi(\cdot, \theta_T)$ must have three local minima, i.e. 'energy-wells', and the value of ψ at these three minima must be the same. The minima occurring at the smallest, intermediate and largest values of polarization intensity are identified with F^-, P and F^+, respectively. Next, we require that the value of ψ at the two ferroelectric

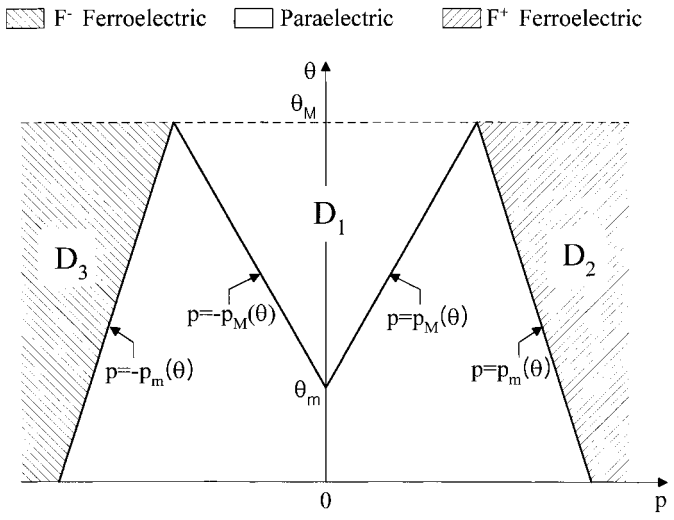

Fig. 2. Regions, D_1, D_2, and D_3 in the (p, θ)-plane.

energy-wells should coincide at every θ at which these energy-wells exist, reflecting the fact that F^+ and F^- are 'variants' of each other. Finally, for $\theta > \theta_T$ the ferroelectric wells must be higher than the paraelectric well, while for $\theta < \theta_T$ they should be lower, so that paraelectric is preferred at higher temperatures, ferroelectric at lower temperatures. The special temperature θ_T is the transformation temperature of paraelectric–ferroelectric phase transformations and is often called the Curie point.

Enforcing these requirements on the function ψ defined by (18) yields

$$\psi_1 - \psi_2 - \frac{\chi\beta^2}{\rho}\frac{\theta_T^2}{2} = \psi_1 - \psi_3 - \frac{\chi\beta^2}{\rho}\frac{\theta_T^2}{2} \equiv \lambda_T > 0, \tag{19}$$

$$\log\left(\frac{\theta_2}{\theta_1}\right) = -\frac{\chi\beta}{\rho c}(p_2 - \beta\theta_T) + \frac{\lambda_T}{c\theta_T},$$

$$\log\left(\frac{\theta_3}{\theta_1}\right) = \frac{\chi\beta}{\rho c}(p_3 + \beta\theta_T) + \frac{\lambda_T}{c\theta_T}. \tag{20}$$

In (19) we have let λ_T denote the common value of $\psi_1 - \psi_2 - (\chi\beta^2/\rho)(\theta_T^2/2)$ and $\psi_1 - \psi_3 - (\chi\beta^2/\rho)(\theta_T^2/2)$; one can readily verify that λ_T represents the *latent heat* of the paraelectric $\rightarrow$ ferroelectric transitions at $\theta = \theta_T$.

The electric field-response function $\hat{e}(p, \theta) = \rho\psi_p(p, \theta)$ associated with (18) is

$$\hat{e}(p, \theta) = \begin{cases} \chi(p - p_1) & \text{on } D_1, \\ \chi(p - p_2) + \chi\beta\theta & \text{on } D_2, \\ \chi(p - p_3) - \chi\beta\theta & \text{on } D_3, \end{cases} \tag{21}$$

Two graphs of $\hat{e}(p, \theta)$ vs p are shown in Fig. 3: Fig. 3 (a) corresponds to a fixed value of temperature in the range $\theta_m < \theta < \theta_M$ and the electric field–polarization curve shows three rising branches

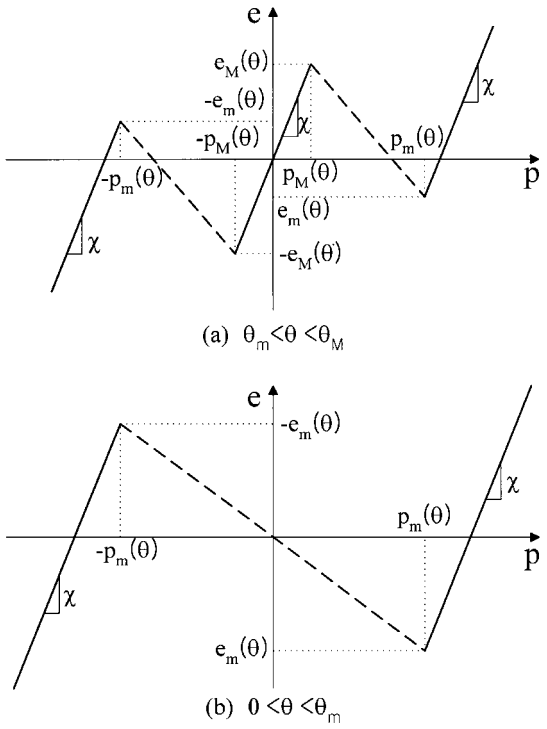

Fig. 3. Electric field–polarization intensity curves at constant temperature θ.

corresponding to the three phases, P, F^+ and F^-; Fig. 3 (b) is associated with a temperature in the range $0 < \theta < \theta_m$ and the two rising branches of the electric field–polarization curve correspond to the variants F^+ and F^-.

Of the three parameters p_1, p_2 and p_3, one is fixed by the choice of reference configuration, while the other two are determined through the transformation polarizations. In particular, if we choose electric field-free paraelectric at the transformation temperature θ_T to be the reference state, then by setting $\hat{e}(0, \theta) = 0$ in $(21)_1$ one obtains

$$p_1 = 0. \tag{22}$$

Next, let $p_T(> 0)$ denote the *transformation polarization intensity* between each ferroelectric variant and paraelectric. Then, from (21),

$$p_T = p_2 - \beta\theta_T = -p_3 - \beta\theta_T > 0. \tag{23}$$

Finally, if (19), (20), (22) and (23) are substituted back into (18), one finds that $\rho\psi(p, \theta)$ contains the term $\rho\psi_1 + \rho c\theta \log(\theta_1/\theta_T)$ as an inessential linear function of temperature which may be eliminated by taking

$$\psi_1 = 0, \quad \theta_1 = \theta_T. \tag{24}$$

The latter condition $\theta_1 = \theta_T$ of (24) implies that the value of specific entropy of paraelectric phase at $\theta = \theta_T$ is taken to be zero.

In summary, the material at hand is characterized by the common inverse susceptibility at constant

temperature χ and specific heat at constant polarization c of the phases; the pyroelectric coefficients 0, $-\beta$ and β of the respective, P, F^+ and F^- phases; the electric field-free transformation temperature θ_T; the mass density ρ in the reference state; the latent heat λ_T at $\theta = \theta_T$ and the transformation polarization intensity p_T. The Helmholtz free-energy function is given by combining (18) with (19), (20), and (22)–(24):

$$\rho\psi(p,\theta) = \begin{cases} (\chi/2)p^2 + \rho c\theta\big(1 - \log(\theta/\theta_T)\big) & \text{on } D_1, \\ (\chi/2)(p-p_T)^2 + \chi\beta(p-p_T)(\theta-\theta_T) + \rho c\theta\big(1-\log(\theta/\theta_T)\big) - \rho\lambda_T(1-\theta/\theta_T), & \text{on } D_2, \\ (\chi/2)(p+p_T)^2 - \chi\beta(p+p_T)(\theta-\theta_T) + \rho c\theta\big(1-\log(\theta/\theta_T)\big) - \rho\lambda_T(1-\theta/\theta_T) & \text{on } D_3. \end{cases} \tag{25}$$

The various other thermoelectrical characteristics of the material can now be derived from (25). In particular, the electric field-response function $\hat{e}(p,\theta) = \rho\psi_p(p,\theta)$ is given by

$$\hat{e}(p,\theta) = \begin{cases} \chi p & \text{on } D_1, \\ \chi(p-p_T) + \chi\beta(\theta-\theta_T) & \text{on } D_2, \\ \chi(p+p_T) - \chi\beta(\theta-\theta_T) & \text{on } D_3. \end{cases} \tag{26}$$

In order to complete the description of the Helmholtz free energy function we need to specify the regions D_1, D_2 and D_3 of the (p, θ)-plane shown in Fig. 2, i.e. we need to specify the boundary curves $p = p_M(\theta)$, $p_m(\theta)$ shown in the figure. To this end, we first prescribe the electric field-levels at the local maxima and minima of the electric field–polarization curve. As indicated in Fig. 3, we take, for simplicity, these electric field-levels to be given by $\pm e_M(\theta)$ and $\pm e_m(\theta)$. In view of our earlier assumption that the boundaries of the regions D_1, D_2 and D_3 are straight, the functions $e_M(\theta)$ and $e_m(\theta)$ must be linear in θ. Moreover, since according to Fig. 2 we must have $\hat{p}_M(\theta_M) = \hat{p}_m(\theta_M)$ and $\hat{p}_M(\theta_m) = 0$, it follows that $e_M(\theta_m) = 0$ and $e_M(\theta_M) - e_m(\theta_M) = \chi\{p_T - \beta(\theta_M - \theta_T)\}$. Thus,

$$\begin{aligned} e_M(\theta) &= \chi M(\theta - \theta_m) && \text{for } \theta_m < \theta < \theta_M, \\ e_m(\theta) &= \chi m(\theta - \theta_M) + \chi M(\theta_M - \theta_m) - \chi\big\{p_T - \beta(\theta_M - \theta_T)\big\} && \text{for } 0 < \theta < \theta_M, \end{aligned} \tag{27}$$

where m and M are positive material constants. The equations $p = p_M(\theta), p_m(\theta)$ describing the boundaries of D_1, D_2 and D_3 are then given by $\pm e_M(\theta) = \hat{e}(\pm p_M(\theta), \theta)$ and $\pm e_m(\theta) = \hat{e}(\pm p_m(\theta), \theta)$.

Thus far, we have only described ψ on the ('metastable') portion $D_1 + D_2 + D_3$ of the (p, θ)-plane. It is not necessary, for the purposes of the present section, to specify an explicit form for ψ on the remaining ('unstable') portion of this plane; any function ψ which is once continuously differentiable, is such that ψ_p is negative on the unshaded portion of Fig. 2, and conforms with (18) would be acceptable. An infinite number of such functions exist, provided only that the material parameters satisfy certain inequalities; this is discussed in the Appendix.

3.2. Stability, driving traction and latent heat

Since electric field and temperature are uniform throughout the bar, it will often be convenient to utilize expressions for the quantities of physical interests in terms of e and θ. Because the relation (26) between the electric field and polarization at fixed θ is not globally invertible, such expressions must be obtained separately for each phase. Inverting (26) gives the polarization intensities related to the electric field through

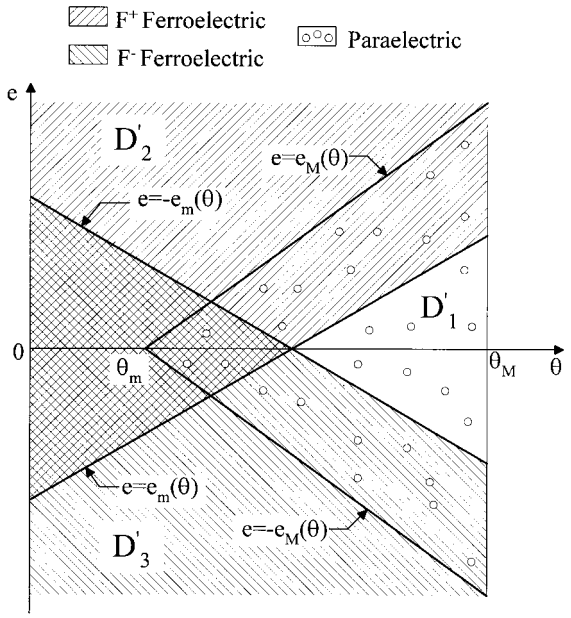

Fig. 4. Available phases at a given (θ, e).

$$\hat{p}(\theta, e) = \begin{cases} e/\chi & \text{on } D_1', \\ e/\chi - \beta(\theta - \theta_T) + p_T & \text{on } D_2', \\ e/\chi + \beta(\theta - \theta_T) - p_T & \text{on } D_3'. \end{cases} \tag{28}$$

where each of the regions D_i', $i = 1, 2, 3$, is obtained from mapping the corresponding regions D_i of the (p, θ)-plane on to the (θ, e)-plane and is displayed in Fig. 4. Given the electric field e and temperature θ at a particle, Fig. 4 shows all of the phases that are available to that particle.

The specific entropy is given, according to (1), (25) and (28), by

$$\hat{\eta}(\theta, e) = \begin{cases} c \log(\theta/\theta_T) & \text{on } D_1', \\ -(\beta e/\rho) + \left(\chi\beta^2/\rho\right)(\theta - \theta_T) + c \log(\theta/\theta_T) - \lambda_T/\theta_T & \text{on } D_2', \\ (\beta e/\rho) + \left(\chi\beta^2/\rho\right)(\theta - \theta_T) + c \log(\theta/\theta_T) - \lambda_T/\theta_T & \text{on } D_3'. \end{cases} \tag{29}$$

The potential energy function $G(p; \theta, e) = \rho\psi(p, \theta) - ep$ of the material at hand can be calculated using (25). At each (θ, e), G has one or more local minima. The values of G at the local minima coincide with the Gibbs free energy per unit reference volume. In terms of θ and e, the Gibbs free-energy per unit reference volume for each phase is obtained by combining (3), (25) and (28):

$$\hat{g}(\theta, e) = \begin{cases} -(1/2\chi)e^2 + \rho c\theta\left(1 - \log(\theta/\theta_T)\right) & \text{on } D_1', \\ -(1/2\chi)\left(e - \chi\beta(\theta - \theta_T)\right)^2 + \rho c\theta\left(1 - \log(\theta/\theta_T)\right) - \rho\lambda_T(1 - \theta/\theta_T) - ep_T & \text{on } D_2', \\ -(1/2\chi)\left(e + \chi\beta(\theta - \theta_T)\right)^2 + \rho c\theta\left(1 - \log(\theta/\theta_T)\right) - \rho\lambda_T(1 - \theta/\theta_T) + ep_T & \text{on } D_3'. \end{cases} \tag{30}$$

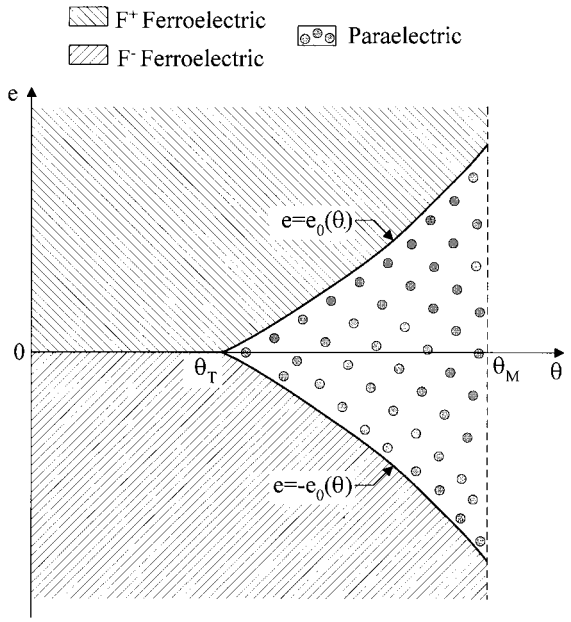

Fig. 5. The stable phases.

Where G has multiple energy-wells, one can use (30) to determine the particular minimum that is smallest. This determines the phase that is stable. The result of this calculation is displayed in Fig. 5. Assuming the $p_T - \beta(\theta - \theta_T) > 0$ for $0 < \theta < \theta_M$, the electric field-level $e_0(\theta)$ indicated in the figure is given by

$$e_0(\theta) = \frac{\rho\lambda_T/\theta_T - (\chi\beta^2/2)(\theta - \theta_T)}{p_T - \beta(\theta - \theta_T)}(\theta - \theta_T), \tag{31}$$

and is known as the *Maxwell* electric field for the $P \leftrightarrow F^+$ transition. The Maxwell electric field for the $P \leftrightarrow F^-$ and $F^+ \leftrightarrow F^-$ transitions are $-e_0(\theta)$ and 0, respectively. One can obtain a Clausius–Clapeyron-like expression by differentiating (31) with respect to temperature and using (28), (29) and (31). The two states P and F^+ that are both associated with any particular point on the boundary $e = e_0(\theta)$ both have the same value of potential energy G and both are stable; if these states coexist and are separated by a phase boundary, the driving force on that interface would be zero and the phases would be in phase equilibrium.

We now turn to the driving traction on a phase boundary. Suppose $x = s(t)$ denote the location at time t of a phase boundary in a bar and the particle on the left of the phase boundary is in phase–i while the particle on the right is in phase-j (recall that $i = 1, 2, 3$, corresponds to phases P, F^+, F^-, respectively). The driving force $f = \hat{g}_j(\theta, e) - \hat{g}_i(\theta, e)$ on an i/j phase boundary can be calculated in terms of θ and e from (30) and (31):

$$f = \{p_T - \beta(\theta - \theta_T)\}(e - e_0(\theta)) \qquad \text{for a } F^+/P \text{ phase boundary,}$$

$$f = -\{p_T - \beta(\theta - \theta_T)\}(e - e_0(\theta)) \qquad \text{for a } P/F^+ \text{ phase boundary,}$$

$$
\begin{aligned}
f &= \{p_T - \beta(\theta-\theta_T)\}(e+e_0(\theta)) && \text{for a } P/F^- \text{ phase boundary,}\\
f &= -\{p_T - \beta(\theta-\theta_T)\}(e+e_0(\theta)) && \text{for a } F^-/P \text{ phase boundary,}\\
f &= 2\{p_T - \beta(\theta-\theta_T)\}e && \text{for a } F^+/F^- \text{ phase boundary,}\\
f &= -2\{p_T - \beta(\theta-\theta_T)\}e && \text{for a } F^-/F^+ \text{ phase boundary.}
\end{aligned} \tag{32}
$$

The expression $\lambda = \theta(\overset{+}{\eta} - \bar{\eta})$, called *latent heat*, represents the heat generated when a unit mass of material transforms from $(\overset{+}{p}, \theta)$ to $(\bar{p}, \theta)$ under a condition of phase equilibrium. The latent heat for various transitions are calculated from (29) in terms of θ and e:

$$
\begin{aligned}
\lambda &= \lambda_T\frac{\theta}{\theta_T} - \frac{\chi\beta^2}{\rho}\theta(\theta-\theta_T) + \frac{\beta}{\rho}\theta e && \text{for } P \to F^+,\\
\lambda &= -\lambda_T\frac{\theta}{\theta_T} + \frac{\chi\beta^2}{\rho}\theta(\theta-\theta_T) - \frac{\beta}{\rho}\theta e && \text{for } F^+ \to P,\\
\lambda &= \lambda_T\frac{\theta}{\theta_T} - \frac{\chi\beta^2}{\rho}\theta(\theta-\theta_T) - \frac{\beta}{\rho}\theta e && \text{for } P \to F^-,\\
\lambda &= -\lambda_T\frac{\theta}{\theta_T} + \frac{\chi\beta^2}{\rho}\theta(\theta-\theta_T) + \frac{\beta}{\rho}\theta e && \text{for } F^- \to P,\\
\lambda &= \frac{2\beta}{\rho}\theta e && \text{for } F^- \to F^+\\
\lambda &= -\frac{2\beta}{\rho}\theta e && \text{for } F^+ \to F^-.
\end{aligned} \tag{33}
$$

Thus, the presence of the electric field does contribute to the generation of heat during a phase transition. In particular heat is generated during $F^- \leftrightarrow F^+$ transitions if the $F^- \to F^+$ transition occurs at a positive value of electric field and the reverse $F^+ \to F^-$ transition at a negative value; however, if it occurs under conditions of phase equilibrium, then from (32) $e = 0$ and the heat generated is zero. The parameter λ_T, as mentioned previously, represents the amount of heat generated when a unit mass of paraelectric transforms to ferroelectric at $\theta = \theta_T$; in the reverse case the same amount of heat disappears.

4. Nucleation and kinetics

Given the electric field e and temperature θ at a particle, Fig. 4 shows the various phases that the particle can adopt, while Fig. 5 indicates which among them is the stable phase. If a particle always chooses the phase that is stable from among all phases available to it, the response of the particle at a

given electric field and temperature is determined by Fig. 5. In solids however, particles can often remain for long times in states that are merely metastable. Therefore, the questions of whether and how fast, it will transform into the stable phase are answered by a nucleation criterion and a kinetic law. A particle changes its phase spontaneously if the electric field and temperature at that particle satisfy an appropriate nucleation criterion; once a new phase is nucleated, the growth of the phase, that is, the motion of the phase boundary is controlled by a kinetic law. Simple models for nucleation and kinetics are developed based on the notion of 'thermal activation' by Abeyaratne and Knowles (1993) and Abeyaratne et al. (1994).

4.1. Nucleation criterion

In this paper, we assume that there exists a critical value of driving traction n_{ij} for the onset of an $i \to j$ phase transformation. Therefore, a particle which is in i phase will transform to j by nucleation if the driving traction $f = \hat{g}_i(\theta, e) - \hat{g}_j(\theta, e)$ is bigger than n_{ij}. In view of the symmetry of the potential energy function G when $e = 0$, we shall assume that both the $P \to F^+$ and $P \to F^-$ transitions nucleate at the same value of temperture if the electric field vanishes; a similar assumption for the reverse $F^+ \to P$ and $F^- \to P$ transitions will also be made. The former value of nucleation temperature is denoted by P_s (for 'paraelectric start') while the latter is denoted by F_s (for 'ferroelectric start'). Finally, we will also assume that at any given temperature θ, the nucleation electric field-level for the $F^+ \to F^-$ transition is the negative of the nucleation electric field-level for the reverse $F^- \to F^+$ transition at the same temperature. One can readily enforce these restrictions on the n_{ij}s, yielding the following *nucleation criteria* for the various transitions:

$$
\begin{aligned}
&e \geqslant e_0(\theta) - e_0(F_s)\frac{p_T - \beta(F_s - \theta_T)}{p_T - \beta(\theta - \theta_T)} && \text{for } P \to F^+,\\
&e \leqslant e_0(\theta) - e_0(P_s)\frac{p_T - \beta(P_s - \theta_T)}{p_T - \beta(\theta - \theta_T)} && \text{for } F^+ \to P,\\
&e \leqslant -e_0(\theta) + e_0(F_s)\frac{p_T - \beta(F_s - \theta_T)}{p_T - \beta(\theta - \theta_T)} && \text{for } P \to F^-,\\
&e \geqslant -e_0(\theta) + e_0(P_s)\frac{p_T - \beta(P_s - \theta_T)}{p_T - \beta(\theta - \theta_T)} && \text{for } F^- \to P,\\
&e \geqslant \frac{N}{2\{p_T - \beta(\theta - \theta_T)\}} && \text{for } F^- \to F^+,\\
&e \leqslant -\frac{N}{2\{p_T - \beta(\theta - \theta_T)\}} && \text{for } F^+ \to F^-,
\end{aligned}
\tag{34}
$$

where $e_0(\theta)$ is the paraelectric-ferroelectric Maxwell electric field given by (31) and the constants F_s, P_s and N are characteristic of the material; necessarily, $F_s < \theta_T < P_s$ and $N > 0$.

Fig. 6 illustrates these nucleation criteria on the (θ, e)-plane. The lines in Fig. 6 correspond to eqns (34) with inequalities replaced by equalities and crossing one of these lines nucleates an associated transition. If the value of energy barrier N between F^+ and F^- is bigger than a critical value, then the

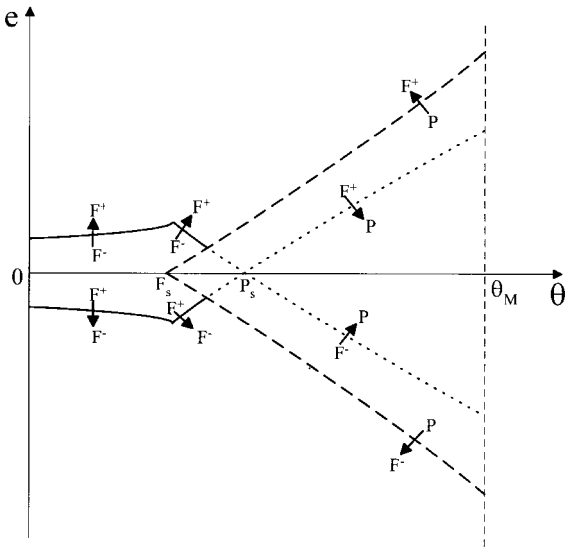

Fig. 6. Nucleation criteria.

critical nucleation electric field-level given by (34) for the $F^- \rightarrow P$ transition exceeds the corresponding electric field-level for the $P \rightarrow F^+$ transition for some range of temperatures, as shown in Fig. 6. This critical value of N, even though it is not shown here, may be obtained from (31) and (34).

Since we will consider a uniform bar which is always subjected to uniform electric and temperature field, there is no preferred site for nucleation. The location for the nucleation in this bar is rather arbitrary. Therefore, for simplicity, we assume that the transition from a low-polarization phase to a high-polarization phase would occur at $x = 0$ and the reverse transition would commence at $x = L$.

4.2. Kinetics

A kinetic relation has been introduced by Abeyaratne and Knowles (1988) to construct a determinate theory of quasi-static motions of a bar which is capable of thermoelastic phase transformations. An example of a kinetic relation which is based on the classical notion of 'thermally activated' phase transitions is constructed in Abeyaratne and Knowles (1993) and used in Abeyaratne et al. (1994) and Kim and Abeyaratne (1995). One may develop a similar continuum model of a kinetic relation governing the propagation of phase boundary in a thermopolarizable solid undergoing thermoelectric phase transformations. In the present study, however, we do not construct a specific model of a kinetic relation. Instead, for simplicity, we shall take the following simple linear kinetic relation for every phase transition:

$$\dot{s} = Rf, \tag{35}$$

where $R > 0$ is a material constant and represents the mobility of phase boundary. The kinetic relation (35) has the form of (15) and therefore, it conforms with the dissipation inequality (12).

5. Thermoelectrical response of the model

In this section we use explicit forms of the Helmholtz free-energy (25), the nucleation criterion (34) and the kinetic relation (35) to study the quasi-static thermoelectrical responses of a bar under various

thermal and electrical loadings. We describe here the analysis associated with one of these loadings in some detail; the analysis corresponding to the remaining cases is conceptually similar.

We consider a uniform bar which is subjected to an electrical cyclic loading at a constant temperature $\theta > F_s$. Initially the bar is composed of a paraelectric phase under no electric field. As the applied electric field $e(t)$ increases monotonically, the bar is in one of the following three states; for some initial time $0 < t < t_1$, the bar is in the paraelectric phase, then the F^+ ferroelectric phase nucleates at the left end of the bar at $t = t_1$ and the phase boundary moves to the right direction, reaching the right end at $t = t_2$, finally, for $t > t_2$, the bar remains in the single F^+ phase. The average polarization intensity $p_a(t)$ for each stage of the phase transformation is given using (28) by

$$p_a(t) = \begin{cases} \dfrac{e(t)}{\chi} & \text{for } 0 < t < t_1, \\ \dfrac{s(t)}{L}\left[\dfrac{e(t)}{\chi} - \beta(\theta(t) - \theta_T) + p_T\right] + \dfrac{L - s(t)}{L}\dfrac{e(t)}{\chi} & \text{for } t_1 < t < t_2, \\ \dfrac{e(t)}{\chi} - \beta(\theta(t) - \theta_T) + p_T & \text{for } t_2 < t, \end{cases} \tag{36}$$

where t_1 is from (34)

$$e(t_1) = e_0(\theta) - e_0(F_s)\frac{p_T - \beta(F_s - \theta_T)}{p_T - \beta(\theta - \theta_T)}. \tag{37}$$

The location of the phase boundary $s(t)$ is found by integrating the kinetic relation (35), i.e.

$$\dot{s}(t) = Rf, \quad s(t_1) = 0, \tag{38}$$

with the driving force $f = [p_T - \beta(\theta - \theta_T)](e(t) - e_0(\theta))$. A similar analysis can be used to describe the response corresponding to subsequent unloading, as well as to loading by negative electric field in which the F^- variant is involved instead of F^+.

In order to compare the predictions of the model with experimental observations, we used values of the material parameters that are of the correct order of magnitude for $BaTiO_3$, except R which is arbitrarily taken so that it produces reasonable responses:

$$p_T = 0.26 \text{ C/m}^2, \quad \chi = 8.037 \times 10^7 \text{ V} \cdot \text{m/C}, \quad c = 523 \text{ J/kg} \cdot {}^\circ\text{K},$$

$$\rho = 5850 \text{ kg/m}^3, \quad \beta = 887 \times 10^{-6} \text{ C/m}^2 \cdot {}^\circ\text{K}, \quad \lambda_T = 897 \text{ J/kg},$$

$$F_s = 392^\circ\text{K}, \quad \theta_T = 393^\circ\text{K}, \quad P_s = 394^\circ\text{K}, \quad N = 51{,}532 \text{ J/m}^3, \quad R = 5 \times 10^{-7} \text{ m}^4/\text{J} \cdot \text{s}. \tag{39}$$

The values of p_T, χ, c, β, λ_T, F_s, θ_T and P_s were taken from Jona and Shirane (1962) and the value of N was estimated using the experimental values of coercive field in Jona and Shirane (1962) and the nucleation criterion (34). The value of ρ was obtained from JCPDS-International Center for Diffraction Data (1995). The length of the bar was chosen to be 5 cm.

Four other material constants, viz m, M, θ_m and θ_M that are involved in the description of our model, but that do not affect its response, should exist in a manner that is consistent with the various constitutive inequalities given in the Appendix. One can show that there is a range of acceptable values for these parameters.

(i) Fig. 7 shows two electric field–polarization intensity curves corresponding to isothermal electrical load cycling. Fig. 7 (a) corresponds to a temperature below F_s, with the bar transforming between the F^- and F^+ variants without involving paraelectric. Fig. 7 (b) corresponds to a temperature above P_s; as the electric field increases from a sufficiently negative value, the bar transforms from F^- to P and then from P to F^+. The electrical loading and unloading rate underlying both of these figures is $|\dot{e}(t)| = 10^6$ V/m · s. The response depicted in these figures is similar to that observed by Merz (1953) for $BaTiO_3$.

(ii) Fig. 8 shows a temperature–polarization intensity curve which results from cycling the temperature with the electric field intensity held fixed at a positive value. The transformation from the high temperature phase (paraelectric) to the low temperature phase (the F^+ variant of ferroelectric phase) involves a positive polarization. Even though we do not show it here, we have found that if the electric field is fixed at a negative value a negative polarization is induced due to the $P \leftrightarrow F^-$ phase transition. The heating and cooling rate underlying the figure is $|\dot{\theta}(t)| = 1^\circ$K/s. Unfortunately experimental observations for comparison are not available at this moment.

(iii) Fig. 9 shows two electric field–polarization curves corresponding to different electrical loading

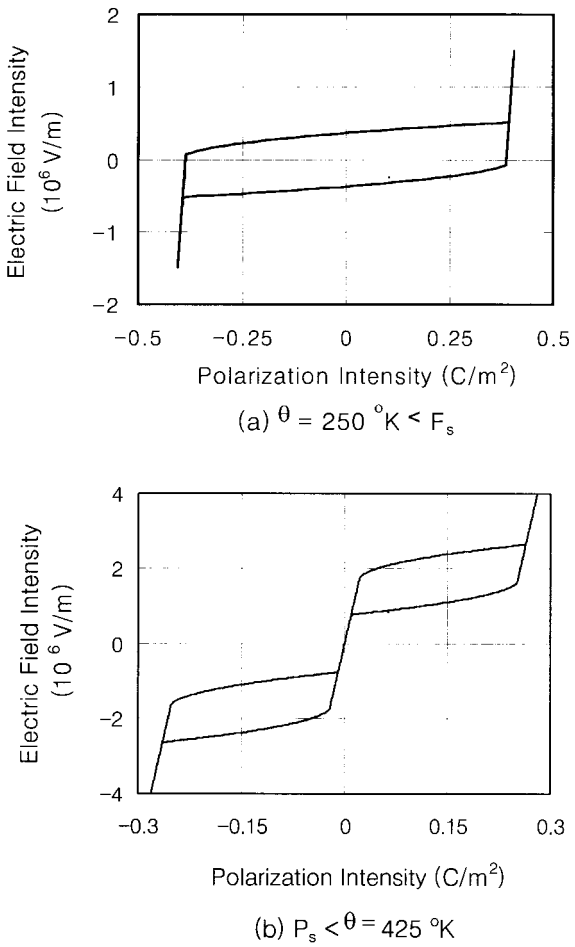

Fig. 7. The electric field–polarization responses at various constant temperatures.

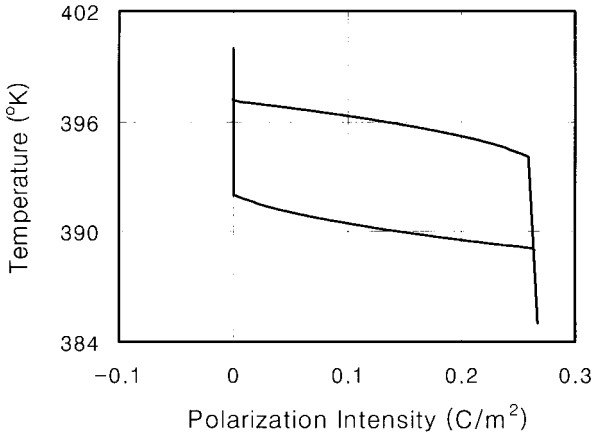

Fig. 8. The temperature–polarization intensity response when the electric field is 5×10^3 V/m · s.

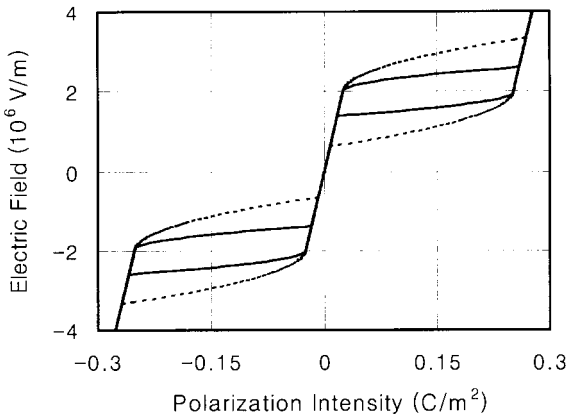

Fig. 9. The electric field–polarization response at different electrical loading rates with the temperature held fixed at $\theta = 430$°K.

rates at a fixed temperature greater than P_s. The solid line represents the response at the electrical loading rate $|\dot{e}(t)| = 4 \times 10^5$ V/m · s; the dotted one corresponds to the response at $|\dot{e}(t)| = 2 \times 10^6$ V/m · s. In the figure we observe that the hysteresis loops increase in area as the electrical loading rate increases. These results may be compared with those of Kim and Abeyaratne (1995) for shape-memory alloys. Though we shall not display it here, we have also carried out similar calculations at a constant temperature below F_s and found that the size of hysteresis loop, i.e. the magnitude of the coercive field, increases as the electrical loading rate increases. This phenomenon has been observed experimentally, e.g. Wieder (1957), Campbell (1957).

(iv) Fig. 10 exhibits the electric field–polarization responses of the bar predicted by the present model at two different temperatures above P_s with the electrical loading rate held fixed. The solid line represents the response at $\theta = 460$°K; the dotted one corresponds to the response at $\theta = 425$°K. We note two principal effects of increasing temperature: one is to shift the hysteresis loop in the direction of increasing the electric field and the other is to decrease the width of the hysteresis loop. The latter is due to the pyroelectric effect of the ferroelectric phase. The response depicted in these figures is similar to the response described by Merz (1953) for $BaTiO_3$.

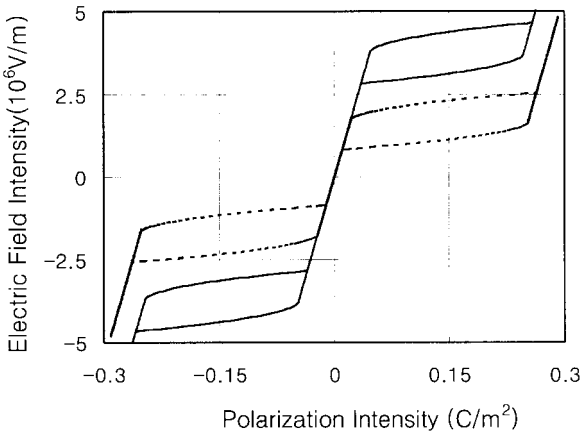

Fig. 10. The electric field–polarization responses at different temperatures with the electrical loading rate held fixed at $|\dot{e}(t)| = 8 \times 10^5$ V/m · s.

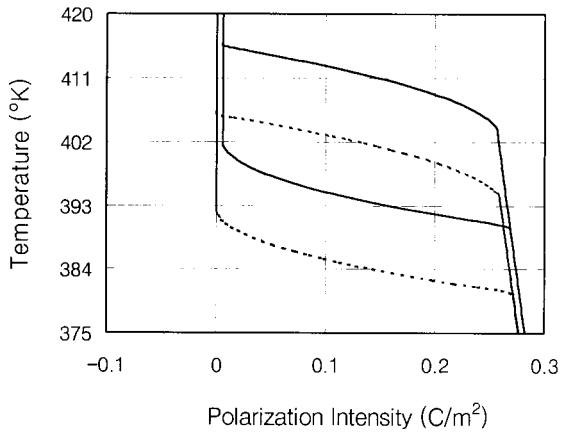

Fig. 11. The temperature–polarization responses at different electric field intensities under the same thermal loading rate $|\dot{\theta}(t)| = 10°\text{K/s}$.

(v) A similar movement of the hysteresis loop is shown in Fig. 11, where the bar is subjected to thermal load cycling with the electric field held fixed. The bar transforms between the phases P and F^+. The solid line represents the response when the electric field intensity is fixed at $e = 5 \times 10^5$ V/m; the dotted one corresponds to the response when $e = 10^4$ V/m. As the electric field gets bigger, the hysteresis loop moves in the upward direction with no significant change in the shape of the hysteresis loop.

Acknowledgement

The authors would like to thank Ji-Hoon Yang, a student of the Department of Mechanical Engineering in the University of Seoul, for carrying out numerical calculations. The research summarized here has been supported by the Korea Science and Engineering Foundation under Grant No. 971-1004-019-2.

Appendix. Restrictions on the material parameters

Here we shall list all of the inequalities not displayed previously which the material parameters must satisfy. According to the statements below (27) the equations of the boundaries of the regions D_i in the (p, θ)-plane are given by

$$p_M(\theta) = e_M(\theta)/\chi \qquad \text{for } \theta_m < \theta < \theta_M,$$

$$p_m(\theta) = e_m(\theta)/\chi + p_T - \beta(\theta - \theta_T) \qquad \text{for } 0 < \theta < \theta_M, \tag{40}$$

where the electric field-levels $e_m(\theta)$ and $e_M(\theta)$ are given by (27). In order that the corresponding straight lines in the (p, θ)-plane be arranged as shown in Fig. 2, it is necessary that $0 < p_M(\theta) < p_m(\theta)$ for $\theta_m < \theta < \theta_M$ and that $0 < p_m(\theta)$ for $0 < \theta < \theta_m$. These inequalities can be expressed, upon using (40), as

$$0 < e_M(\theta) < e_m(\theta) + \chi p_T - \chi\beta(\theta - \theta_T) \qquad \text{for } \theta_m < \theta < \theta_M,$$

$$0 < e_m(\theta) + \chi p_T - \chi\beta(\theta - \theta_T) \qquad \text{for } 0 < \theta < \theta_m. \tag{41}$$

Since we assumed in Section 3 that all three phases F^-, P and F^+ exist when $e = 0$ and $\theta = \theta_T$, it is necessary that the corresponding polarization intensities $p = -p_T$, 0, p_T lie in the appropriate polarization ranges as defined by Fig. 2. In view of (40) and (41), one finds that this holds if and only if

$$e_m(\theta_T) < 0. \tag{42}$$

In deriving (31) it is assumed that

$$p_T - \beta(\theta - \theta_T) > 0 \quad \text{for } 0 < \theta < \theta_M. \tag{43}$$

We turn finally to the issue of extending the Helmholtz free-energy function (25) to the unshaded ('unstable') region of the (p, θ)-plane shown in Fig. 2. In order to show the extendibility of ψ on this region, we must show that each adjacent pair of rising branches of the electric field–polarization curve in Fig. 3 can be connected by a declining branch with a prescribed area under it. Since the electric field–polarization curve is to be declining on the unstable regions in Fig. 2, it is necessary that

$$e_m(\theta) < e_M(\theta) \quad \textit{for } \theta_m < \theta < \theta_M, \quad e_m(\theta) < -e_m(\theta) \quad \text{for } 0 < \theta < \theta_m. \tag{44}$$

Next, as is readily seen from Fig. 3(a), for $\theta_m < \theta < \theta_M$, the area under the graph of $\hat{e}(\bullet, \theta)$ between $p = \hat{p}_M(\theta)$ and $p = \hat{p}_m(\theta)$, must necessarily lie between the areas of the two rectangles with the same bases $(p_M(\theta), p_m(\theta))$ and with heights $e_M(\theta)$ and $e_m(\theta)$. A similar restriction applies to the area between $p = -\hat{p}_m(\theta)$ and $p = -\hat{p}_M(\theta)$ and for $0 < \theta < \theta_m$ to the area between $p = -\hat{p}_m(\theta)$ and $p = \hat{p}_m(\theta)$. Thus, it is necessary that

$$e_M(\theta)\big(p_M(\theta) - p_m(\theta)\big) < \rho\psi\big(-p_M(\theta), \theta\big) - \rho\psi\big(-p_m(\theta), \theta\big) < e_m(\theta)\big(p_M(\theta) - p_m(\theta)\big),$$

$$e_m(\theta)\big(p_m(\theta) - p_M(\theta)\big) < \rho\psi\big(p_m(\theta), \theta\big) - \rho\psi\big(p_M(\theta), \theta\big) < e_M(\theta)\big(p_m(\theta) - p_M(\theta)\big),$$

$$2e_m(\theta)p_m(\theta) < \rho\psi\big(p_m(\theta), \theta\big) - \rho\psi\big(-p_m(\theta), \theta\big) < -2e_m(\theta)p_m(\theta), \tag{45}$$

where the first two sets of inequalities in (45) hold for $\theta_m < \theta < \theta_M$, while the last set holds for $0 < \theta < \theta_m$. Conversely, given two points $(p_M(\theta), e_M(\theta))$ and $(p_m(\theta), e_m(\theta))$ in the (p, e)-plane, with

$p_m(\theta) > p_M(\theta)$, a sufficient condition for the existence of a continuous decreasing function $\hat{e}(\bullet, \theta)$ connecting these two points, which is such that the area under it is $\rho\psi(p_m(\theta), \theta) - \rho\psi(p_M(\theta), \theta)$, is that $(44)_1$ and $(45)_2$ hold. The requirements (44) and (45) are, therefore, necessary and sufficient for the extendibility of the Helmholtz free-energy function (25) to the unstable region.

The inequalities (45) can be expressed equivalently in terms of the electric fields $e_m(\theta)$, $e_M(\theta)$ and $e_0(\theta)$ as

$$\begin{aligned}
&\big\{e_M(\theta) - e_m(\theta)\big\}^2 < 2\chi\big\{p_T - \beta(\theta - \theta_T)\big\}\big\{e_0(\theta) - e_m(\theta)\big\} && \text{for } \theta_m < \theta < \theta_M,\\
&\big\{e_M(\theta) - e_m(\theta)\big\}^2 < 2\chi\big\{p_T - \beta(\theta - \theta_T)\big\}\big\{e_M(\theta) - e_0(\theta)\big\} && \text{for } \theta_m < \theta < \theta_M,\\
&-\chi\big\{p_T - \beta(\theta - \theta_T)\big\} < e_m(\theta) < 0 && \text{for } 0 < \theta < \theta_m. \qquad (46)
\end{aligned}$$

The inequalities (41)–(44) and (46), which must be enforced on the material parameters, can be reduced into temperature-independent inequalities that involve only the material parameters. One can show that the particular values (39) of the material constants, together with a range of values of the four remaining parameters m, M, θ_m and θ_M, do satisfy these inequalities. For example, one set of values of the latter four parameters is $m = 4 \times 10^{-4}$ C/m$^2 \cdot {}^\circ$K, $M = 1.357833 \times 10^{-3}$ C/m$^2 \cdot {}^\circ$K, $\theta_m = 380^\circ$K and $\theta_M = 500^\circ K$. The particular values of these four material constants do not affect the response of the material.

References

Abeyaratne, R., Knowles, J.K., 1988. On the dissipative response due to discontinuous strains in bars of unstable elastic material. Int. J. Solids Struct. 24, 1021–1042.

Abeyaratne, R., Knowles, J., 1990. On the driving traction acting on a surface of strain discontinuity in a continuum. J. Mech. Phys. Solids 38, 345–360.

Abeyaratne, R., Knowles, J., 1993. A continuum model of a thermoelastic solid capable of undergoing transitions. J. Mech. Phys. Solids 41, 541–571.

Abeyaratne, R., Kim, S.J., Knowles, J., 1994. A one-dimensional continuum model for shape-memory alloys. Int. J. Solids Struct. 31, 2229–2249.

Campbell, D.S., 1957. J. Electronics and Control 3, 330.

Hwang, S.C., Lynch, C.S., McMeeking, R.M., 1995. Ferroelectric/ferroelastic interactions and a polarization switching model. Acta. Metall. Mater. 5, 2073–2084.

JCPDS-International Center for Diffraction Data, 1995. No. 34-129.

Jiang, Q., 1993. Macroscopic behavior of a bar undergoing the paraelectric–ferroelectric phase transformation. J. Mech. Phys. Solids 41, 1599–1635.

Jiang, Q., 1994a. On modeling of phase transformations in ferroelectric materials. Acta Mechanica 102, 149–165.

Jiang, Q., 1994b. On the driving traction acting on a surface of discontinuity within a continuum in the presence of electromagnetic fields. J. Elasticity 34, 1–21.

Jona, F., Shirane, G., 1962. Ferroelectric Crystals. Pergamon Press, New York.

Kim, S.J., Abeyaratne, R., 1995. On the effect of the heat generated during a stress-induced thermoelastic phase transformation. Cont. Mech. Thermo. 7, 311–332.

Kim, S.J., Jiang, Q., 1996. Microcracking and electric fatigue of polycrystalline ceramics. J. Smart. Mat. Struct. 5, 321–326.

McMeeking, R.M., Hwang, S.C., 1996. On the potential energy of a piezoelectric inclusion and the criterion for ferroelectric switching.

Merz, W.J., 1953. Phys. Rev. 91, 513.

Wieder, H.H., 1957. J. Appl. Phys. 28, 367.